

Low Temperature ^1H -, ^{19}F -, and ^{31}P -PGSE Diffusion Measurements. Applications to Cationic Alcohol Complexes

by Eloísa Martínez-Viviente and Paul S. Pregosin*

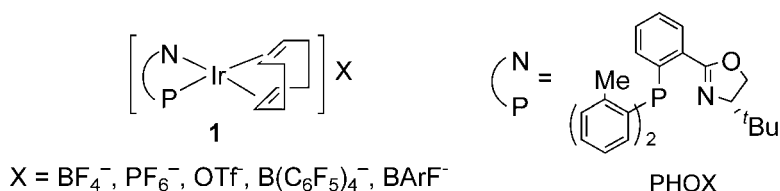
Laboratory of Inorganic Chemistry, ETHZ, Hönggerberg, CH-8093 Zürich
(tel.: +41 1 632 2915; fax: +41 1 632 1090; e-mail: pregosin@inorg.chem.ethz.ch)

The problems associated with low-temperature pulsed-gradient spin-echo (PGSE) NMR diffusion measurements are discussed. The influence of convection is overcome by employing a coaxial insert inside a normal 5 mm NMR tube. By means of this configuration, correct diffusion constants and temperature-independent hydrodynamic radii can be obtained. Low-temperature ^1H -, ^{19}F -, and ^{31}P -PGSE measurements on unstable cationic alcohol complexes of palladium and tungsten (in MeOH and CH_2Cl_2) are reported. For $[\text{W}(\text{Cp})(\text{adamant-1-ol})(\text{CO})_3](\text{CF}_3\text{SO}_3)$, a strong hydrogen bond between the alcohol OH group and the trifluoromethanesulfonate anion is demonstrated.

Introduction. – There are increasing numbers of applications of pulsed-gradient spin-echo (PGSE) NMR diffusion measurements [1][2] in inorganic and organometallic chemistry [3–15]. The calculated diffusion coefficient D can be used to estimate molecular volumes (the larger the molecule, the slower it diffuses).

In recent PGSE diffusion studies, the potential of this technique for the study of ion pairing has been emphasized [16–19]. Through a separate analysis of the translational properties of cation and anion, it is possible to gain insight into whether these charged species move independently or as a single unit in solution. Solvents with a relatively low dielectric constant, such as CHCl_3 , favor the formation of tight ion pairs [18][19]. In these solvents, both cation and anion have been found to show the same, relatively small, diffusion coefficient as they move together as a relatively large unit. In more polar solvents, such as MeOH, the cation and anion are usually not associated and show different and mutually independent D -values. In CH_2Cl_2 , we have observed an intermediate situation, where there is partial but usually not complete ion pairing [18][19]. The translational properties of the cation will then be affected by the anion, and *vice versa*. For salts of transition metals, the PGSE diffusion methodology, frequently in combination with NOE data, offers a unique structural approach to this problem. By means of these methods, the relative anion-dependent activity of the Ir phosphinoxazoline (PHOX) complexes **1** in the catalytic hydrogenation of olefins in CH_2Cl_2 can be explained [6][19][20].

When no ^1H resonances are available in the anion, as in the commonly used BF_4^- , PF_6^- , or trifluoromethanesulfonate (CF_3SO_3^- ; TFMS), a multinuclear approach can be used, with ^{19}F - and ^1H -PGSE diffusion measurements for the cation and anion, respectively. In addition, we have recently shown that ^{31}P is a reliable alternative to ^1H as a diffusion probe in organometallic complexes [18]. ^{31}P -Nuclei can be useful when no suitable ^1H - or ^{19}F -resonances are available, or when it would be preferable to make



measurements in a routine protonated solvent rather than a deuterated one. The diffusion methodology can also be applied to ³⁵Cl in the ClO₄⁻ anion [18].

PGSE Measurements make use of a spin-echo sequence with incorporated pulsed-field gradients, as shown in *Fig. 1, a* for the *Stejskal-Tanner* sequence [1][2]. Moving molecules cause attenuated signal intensities, since they diffuse from their original environment *via* Brownian motion, and, thus, no longer experience the same field strength when the second refocusing gradient is applied. *Eqn 1* relates the observed intensity changes, $\ln(I/I_0)$, as a function of the variables used:

$$\ln\left(\frac{I}{I_0}\right) = -(\gamma\delta)^2\left(\Delta - \frac{\delta}{3}\right)DG^2 \quad (1)$$

where γ = gyromagnetic ratio of the observed nucleus, δ = length of the gradient pulse, G = gradient strength, Δ (diffusion delay) = delay between the midpoints of the gradients, and D = diffusion coefficient.

The D value can be determined from the slope of the regression line $\ln(I/I_0)$ vs. G^2 . A frequently employed modification of the *Stejskal-Tanner* sequence, the so-called stimulated-echo experiment (*Fig. 1, b*), splits the π pulse into two $\pi/2$ pulses [2].

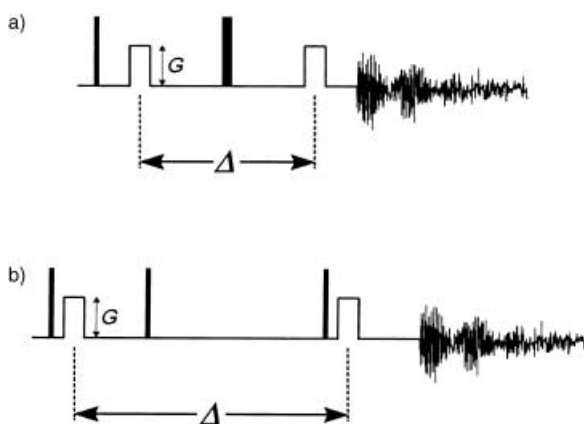
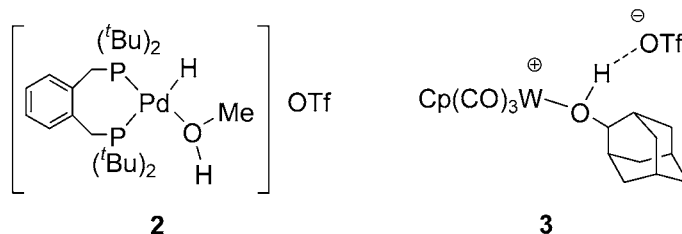


Fig. 1. a) Stejskal-Tanner pulse sequence for NMR PGSE diffusion measurements. The broader open bars represent the gradient pulses and the thin dark bars the hard pulses (90°, thin, and 180°, broad). b) Stimulated echo sequence, obtained by splitting the π pulse in two $\pi/2$ pulses.

Most PGSE diffusion experiments have been carried out at ambient temperature. However, for some applications, it is necessary to measure at higher [21–24] or lower temperatures [25–27]. The latter would be the case for inorganic or organometallic complexes that are fluxional or unstable in solution at ambient temperature, a common observation. The heating or cooling of the sample may have, potentially, two negative effects on diffusion measurements [22–24]. First, it can affect the mechanical stability of the experimental set-up, which is obviously detrimental¹⁾. Second, it may cause the formation of convection currents within the sample, which can be mistaken for faster diffusion, or even completely distort the shape of the $\ln(I/I_0)$ vs. G^2 plot [23].

Convection currents are caused by small temperature gradients within the sample [28], which are difficult to eliminate even in advanced probe designs [22]. Convection introduces an interfering flow-velocity-dependent phase factor into the amplitude dependence of the signals in PGSE experiments [22]. It has been suggested that convection is especially problematic at higher temperatures [22–24]. Interestingly, in some low-temperature PGSE diffusion measurements, convection is not mentioned as a problem [25–27]. In this report, we discuss how convection interferes with the determination of D values *via* PGSE diffusion measurements at low temperature, and how we have overcome the problem. Further, we discuss two applications that involve possible H-bonding effects in the organometallic cationic alcohol complexes **2** and **3**, both of which are unstable at ambient temperature.



Results and Discussion. – *Convection in Low-Temperature PGSE Diffusion Measurements.* Our initial experiments involved model compound **4**, for which low-temperature PGSE diffusion measurements afforded very distorted plots of $\ln(I/I_0)$ vs. G^2 . We reproduce one example in *Fig. 2*. The result was similar for solutions in CD_2Cl_2 , CD_3OD , and (D_8) -toluene. *Hedin* and *Furó* [23] have suggested that convection induces a gradient-dependent lineshape distortion that results in nonlinear plots of $\ln(I/I_0)$ vs. G^2 . As their description was in agreement with our observations (both lineshape distortions and the consequent nonlinear plot), we have identified convection as the origin of our problem²⁾.

- 1) For this reason, we always carry out the diffusion measurements (at ambient temperature) with the airflow disconnected.
- 2) The lineshape distortions and the resulting nonlinear plots do not seem to be related to shaking of the NMR tube due to the N_2 flow, as they do not appear in ambient-temperature measurements with the airflow connected.

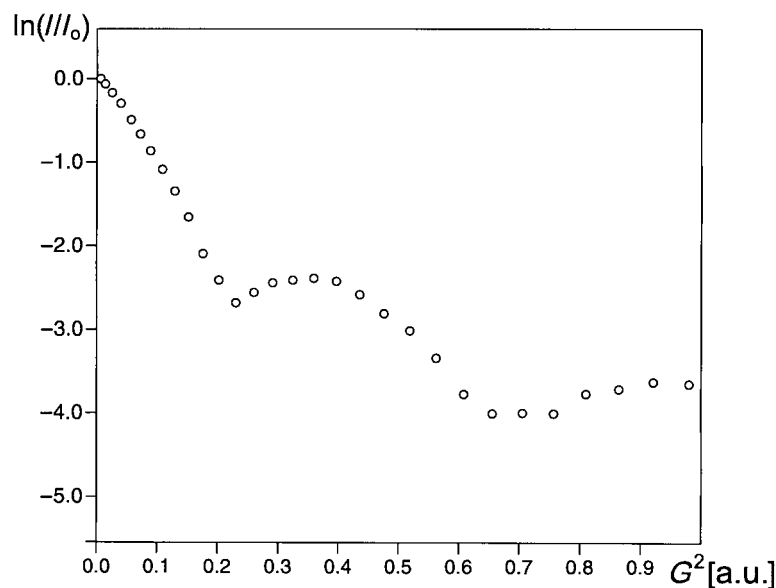
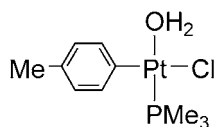


Fig. 2. Plot of $\ln(I/I_0)$ vs. arbitrary units proportional to the square of the gradient amplitude for a ^1H -PGSE diffusion measurement on a 20 mM (D_8)toluene solution of **4**, at 228 K in a 5 mm NMR tube ($\Delta = 68$ ms, $\delta = 2$ ms). The lack of linearity in the plot depends on the parameters used. For $\Delta = 28$ ms and $\delta = 2$ ms, the curvature was much less pronounced, while for $\Delta = 30$ ms and $\delta = 4$ ms, it became significant again.




4

For a given sample with a particular set of properties (viscosity, thermal diffusivity, thermal expansion coefficient), convection appears when the temperature gradient within the solution exceeds a certain level [23][24][29]. It is known that, for cylindrical samples (e.g., in NMR tubes), this value is inversely proportional to the fourth power of the radius of the sample tube [24]. Thus, the obvious way to suppress convection artifacts seems to be to use narrower sample tubes, and this is the approach that we have taken.

However, convection does not necessarily *always* change the character of the signal decay in diffusion experiments. Nonlinearity occurs only when the effect of convection dominates relative to diffusion [24]. Thus, it may happen that linear plots of $\ln(I/I_0)$ vs. G^2 are obtained that, when used together with Eqn. 1, afford incorrect (too large) diffusion coefficients. A sensitive test for the onset of convection is a comparison of D values measured with different diffusion delays (Δ), as convection shows up as Δ -dependent (apparent) diffusion coefficient (D_{app}) [21][23][30]. The longer the duration of Δ , the larger the error in the D_{app} obtained.

Preliminary Experiments. An experimental set-up consisting of two coaxial NMR tubes was chosen. The outer one is a normal 5-mm NMR tube, whereas, for the inner tube we have tested three commercially available inserts, which we will call Small (*S*), Medium (*M*) and Large (*L*), as shown in Fig. 3.



	ID [mm]	OD [mm]
Large (L)	2.34	3.30
Medium (M)	1.96	2.97
Small (S)	1.50	2.52

Fig. 3. Schematic drawing of the experimental set-up used for the low-temperature diffusion measurements, consisting of two coaxial NMR tubes separated by a spacer. ID: inner diameter, OD: outer diameter (both of the internal tube). The outer tube is a normal 5 mm NMR tube.

One would expect a reduction in the temperature gradient within the sample by filling the empty space between the tubes with a liquid that has a higher heat capacity than air [23]³⁾. For this purpose, we chose (*D*₈)toluene. However, as will be shown below, leaving the space between the tubes empty (filled with air) afforded better results.

For the ¹H-PGSE low-temperature test experiments, we chose again complex **4**, which shows a sharp *p*-tolyl methyl ¹H-resonance suitable for fast measurements. These experiments were focused on the two solvents of interest for **2** and **3** (CD₃OD and CD₂Cl₂). We begin the discussion with the results obtained with the three different coaxial inserts (*L*, *M*, and *S*) and air in the intermediate space. The diffusion data for **4** at ambient temperature are shown in Table I. As usual, the hydrodynamic radii (*r*_H) are calculated from the *D* values according to the Stokes–Einstein equation, Eqn. 2 [31]⁴⁾:

$$r_{\text{H}} = \frac{kT}{6\pi\eta D} \quad (2)$$

where *k* = Boltzmann constant, *T* = temperature, *η* = viscosity of the solvent.

³⁾ Hedin et al. [23][24] have used a bath of a perfluorinated oil (between a 5-mm tube and a 10-mm tube) to obtain a delay in the onset of convection in their high-temperature diffusion experiments.

⁴⁾ It has been suggested that the factor 6 in Eqn. 2 is not valid for small species whose Van der Waals radii are < 5 Å [31]. To be consistent and to facilitate comparisons we have used Eqn. 2 as shown. The temperature-dependent equations for the viscosities (of nondeuterated solvents) have been taken from [32]. The calculated hydrodynamic radii (*r*_H) allow comparison of measurements carried out in different solvents or at different temperatures.

Table 1. *D* Values and Calculated r_H Values for **4** at 299 K in CD_3OD and CD_2Cl_2 ^a

Nucleus	CD_3OD ^b		CD_2Cl_2 ^c	
	<i>D</i> [$10^{-10} m^2 s^{-1}$]	r_H [Å]	<i>D</i> [$10^{-10} m^2 s^{-1}$]	r_H [Å]
¹ H	9.45(6)	4.3	12.58(6)	4.2

^a) 20 mm. ^b) η (MeOH) = 0.533 kg s⁻¹ m⁻¹. ^c) η (CH₂Cl₂) = 0.414 kg s⁻¹ m⁻¹.

The low-temperature measurements with configuration (*L*) afforded linear plots, but the *D* values increased markedly with increasing Δ , both for CD_3OD and for CD_2Cl_2 , as shown in Table 2 and Figs. 4 and 5. Consequently, there seems to be a significant contribution of convection to the calculated *D* values. The calculated r_H values are always smaller than at ambient temperature, which is another indication of faster movement due to convection.

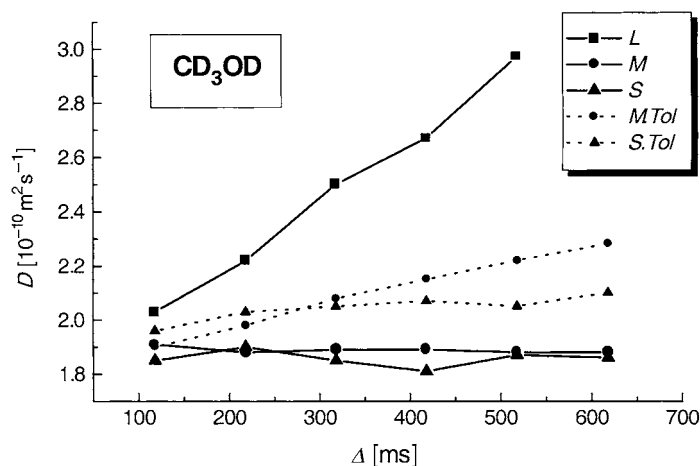


Fig. 4. Measured *D*-value vs. Δ (diffusion delay) for ¹H-PGSE diffusion measurements on CD_3OD solutions of **4** (20 mm) at 228 K with different types of coaxial NMR tubes (see Fig. 3), with air (*L*, *M*, *S*) or (*D_s*)-toluene (*M.Tol* and *L.Tol*) in the intermediate space. The graphs correspond to the data in Tables 2, 3, 4 and 5.

With configuration (*M*), the results were satisfactory for both solvents (see Table 3 and Figs. 4 and 5). The contribution of convection to the calculated *D* values seems to be negligible, and the r_H values are similar to those calculated from measurements at ambient temperature (Table 1)⁵). Positive results were also observed with the (*S*) configuration (Table 4 and Figs. 4 and 5), although the *D* values in (*S*) are slightly lower than in (*M*), which might be an indication of some residual convection in (*M*). This small deviation between (*M*) and (*S*) is larger for CD_2Cl_2 than for CD_3OD . The measurements with the (*M*) and (*S*) configurations are reproducible within ± 2 –3%

⁵) The coincidence of the r_H values calculated from low-temperature and ambient-temperature measurements indicates that there is no significant effect from possible shaking of the NMR tube due to the cold N₂ flow. In ambient temperature measurements, with the airflow connected, the *D* values are, on the contrary, higher than without airflow (smaller r_H values), being these deviations Δ -dependent (more important for higher Δ values).

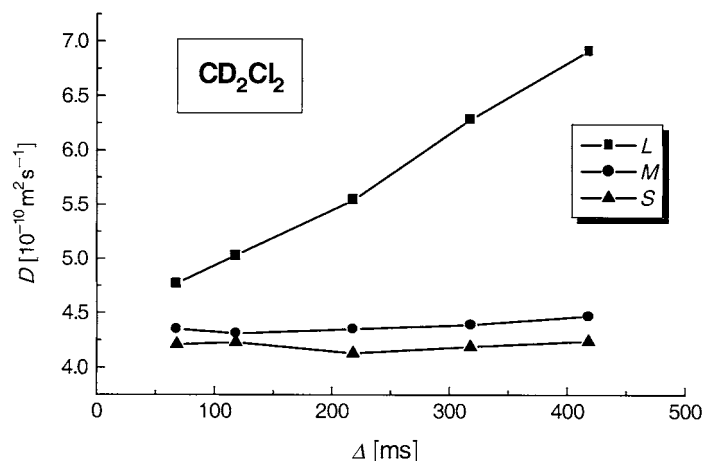


Fig. 5. Measured D value vs. Δ (diffusion delay) for ^1H -PGSE diffusion measurements on CD_2Cl_2 solutions of **4** (20 mm) at 231 K, with different types of coaxial NMR tubes (see Fig. 3), with air in the intermediate space. The graphs correspond to the data in Tables 2, 3 and 4.

Table 2. Low-Temperature ^1H -PGSE Diffusion Results for **4** in L^a

Δ (ms)	$\text{CD}_3\text{OD}^{\text{b}}$		$\text{CD}_2\text{Cl}_2^{\text{c}}$	
	D [$10^{-10} \text{ m}^2 \text{ s}^{-1}$]	r_{H} [\AA]	D [$10^{-10} \text{ m}^2 \text{ s}^{-1}$]	r_{H} [\AA]
68			4.77(6)	3.8(1)
118	2.03(6)	3.9(1)	5.03(6)	3.6(1)
218	2.22(6)	3.6(1)	5.54(6)	3.3(1)
318	2.50(6)	3.2(1)	6.28(6)	2.9(1)
418	2.67(6)	3.0(1)	6.91(6)	2.6(1)
518	2.97(6)	2.7(1)		

^a) 20 mm. ^b) 228 K; η (MeOH) = 2.11 kg s⁻¹ m⁻¹. ^c) 231 K; η (CH₂Cl₂) = 0.933 kg s⁻¹ m⁻¹.

(usually less), while the variations in the measurements with L were sometimes larger (up to ca. 10%).

Clearly, the (L) configuration is not adequate for reliable low-temperature PGSE diffusion measurements, while there does not seem to be a significant difference between the use of the (M) and (S) inserts. Whenever sensitivity is a problem (e.g., for ^{31}P -PGSE diffusion measurements), (M) would be the preferred configuration, as it allows the analysis of a higher volume of sample. In other cases, (S) should be used for best results.

Filling the intermediate space between the tubes with (D_8)toluene gave invariably poorer results. This is shown by test measurements with **4** in CD_3OD (Table 5 and Figs. 4 and 5). For (L), nonlinear plots were obtained when $\Delta \geq 218$ ms. Even when the decay of intensities was linear ($\Delta = 118$ ms), the D value was considerably larger than for the same measurement without (D_8)toluene. For (M) and (S), linear plots were

Table 3. *Low-Temperature ¹H-PGSE Diffusion Results for 4 in M^a*

Δ (ms)	CD ₃ OD ^b		CD ₂ Cl ₂ ^c	
	D [10 ⁻¹⁰ m ² s ⁻¹]	r_H [Å]	D [10 ⁻¹⁰ m ² s ⁻¹]	r_H [Å]
68			4.35(6)	4.2(1)
118	1.91(6)	4.1(1)	4.31(6)	4.2(1)
218	1.88(6)	4.2(1)	4.35(6)	4.2(1)
318	1.89(6)	4.2(1)	4.39(6)	4.1(1)
418	1.89(6)	4.2(1)	4.47(6)	4.1(1)
518	1.88(6)	4.2(1)		
618	1.88(6)	4.2(1)		

^a) 20 mm. ^b) 228 K; η (MeOH) = 2.11 kg s⁻¹ m⁻¹. ^c) 231 K; η (CH₂Cl₂) = 0.933 kg s⁻¹ m⁻¹.

Table 4. *Low-Temperature ¹H-PGSE Diffusion Results for 4 in S^a*

Δ (ms)	CD ₃ OD ^b		CD ₂ Cl ₂ ^c	
	D [10 ⁻¹⁰ m ² s ⁻¹]	r_H [Å]	D [10 ⁻¹⁰ m ² s ⁻¹]	r_H [Å]
68			4.21(6)	4.3(1)
118	1.85(6)	4.3(1)	4.23(6)	4.3(1)
218	1.90(6)	4.3(1)	4.13(6)	4.4(1)
318	1.85(6)	4.3(1)	4.19(6)	4.3(1)
418	1.81(6)	4.4(1)	4.24(6)	4.3(1)
518	1.87(6)	4.2(1)		
618	1.86(6)	4.3(1)		

^a) 20 mm. ^b) 228 K; η (MeOH) = 2.11 kg s⁻¹ m⁻¹. ^c) 231 K; η (CH₂Cl₂) = 0.933 kg s⁻¹ m⁻¹.

Table 5. *Low-Temperature ¹H-PGSE Diffusion Results for 4 in CD₃OD with L, M, or S and (D₈) Toluene^a)^b*

Δ (ms)	L		M		S	
	D [10 ⁻¹⁰ m ² s ⁻¹]	r_H [Å]	D [10 ⁻¹⁰ m ² s ⁻¹]	r_H [Å]	D [10 ⁻¹⁰ m ² s ⁻¹]	r_H [Å]
118	2.40(6)	3.3(1)	1.90(6)	4.2(1)	1.96(6)	4.0(1)
218			1.98(6)	4.0(1)	2.03(6)	3.9(1)
318			2.08(6)	3.8(1)	2.05(6)	3.9(1)
418			2.15(6)	3.7(1)	2.07(6)	3.8(1)
518			2.22(6)	3.6(1)	2.05(6)	3.9(1)
618			2.28(6)	3.5(1)	2.10(6)	3.8(1)

^a) 20 mm. ^b) 228 K; η (MeOH) = 2.11 kg s⁻¹ m⁻¹.

obtained; however, the D values increased with increasing Δ (although this error was not so marked as with (L) and air between the tubes, see *Fig. 4*).

Fig. 6 shows a visual summary of the results obtained from similar ¹H-PGSE diffusion measurements on **4** in different configurations: 5-mm NMR tube (strongly nonlinear), (L) with a (D_8)toluene bath (nonlinear), (L) with air (linear, but incorrect slope), and (M) and (S) with air (correct slopes).

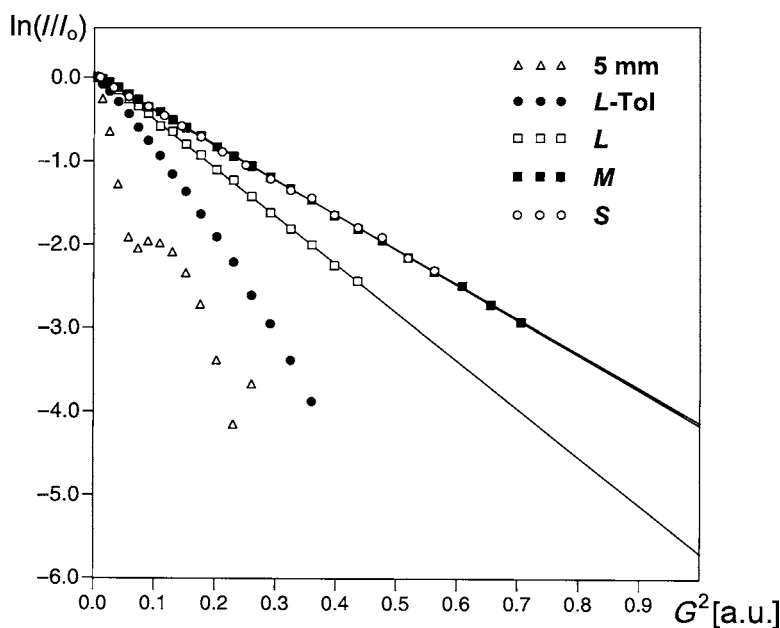


Fig. 6. Plots of $\ln(I/I_0)$ vs. arbitrary units proportional to the square of the gradient amplitude for several ^1H -PGSE diffusion measurements on a 20 mm CD_3OD solution of **4**, at 228 K in a) 5 mm NMR tube (triangles), b) L with a (D_8)toluene bath (filled circles), c) L with air (open squares), d) M with air (filled squares) and e) S with air (open circles). All measurements were carried out with the same diffusion parameters ($\Delta = 318$ ms, $\delta = 1.75$ ms)

We conclude that, although convection is a problem in low-temperature PGSE diffusion measurements, it may be overcome, and reliable D values are obtainable.

Low-Temperature Diffusion Measurements on 2. The Pd^{II} -hydride **2** is thought to be the active catalyst in the Pd-catalyzed methoxycarbonylation of ethene to methylpropanoate, where MeOH is the solvent of choice [33]. Stable Pd hydride complexes are very rare, and almost never occur with the hydride *trans* to P in square-planar complexes. Given the additional dynamics that might arise from solvent exchange, the relative stability of **2** is noteworthy. One might think that, perhaps, the CF_3SO_3^- anion coordinates and/or stabilizes **2** via H-bonding to the complexed solvent molecule.

According to the literature, complex **2** can be generated by dissolving $[\text{Pd}(\text{d}^t\text{bpx})(\text{CF}_3\text{SO}_3)_2]$, **4**, ($\text{d}^t\text{bpx} = 1,2\text{-(CH}_2\text{P}^t\text{Bu}_2)_2\text{C}_6\text{H}_4$) in carefully dried MeOH under N_2 [33c]. However, in our hands, in CD_3OD , a precipitate formed. The ^1H -NMR spectrum of the supernatant solution showed a broad and complicated signal in the Me region, and a diffusion measurement under these conditions did not seem promising. In addition, **2** decomposes slowly in solution, even in nondeuterated MeOH. Since the authors report their NMR data in MeOH [33b,c], we decided to carry out the diffusion studies in this solvent at 240 K (where the compound is stable for prolonged periods) with ^{31}P (instead of ^1H) as a diffusion probe for the cation.

The $^{31}\text{P}\{^1\text{H}\}$ -NMR spectrum of **2** consists of a AX spin system ($\delta(^{31}\text{P}) = 25.8$ and 77.5 ppm, $^2J(\text{P,P}) = 17$ Hz). We have found that the best results, in terms of shape and

intensity of the ^{31}P signals detected, are obtained with the *Stejskal–Tanner* sequence (Fig. 1,a), setting the evolution time before and after the 180° pulse to $1/2 J(\text{P,P}) = 29$ ms.

Fig. 7 shows the good quality of the plots obtained from the ^{31}P and ^{19}F (for the anion) low-temperature diffusion measurements on **2**. Values of D and r_{H} are shown in Table 6. The results show that the cation and anion are moving at very different rates. Clearly, there is no strong H-bond between cation and anion in **2**.

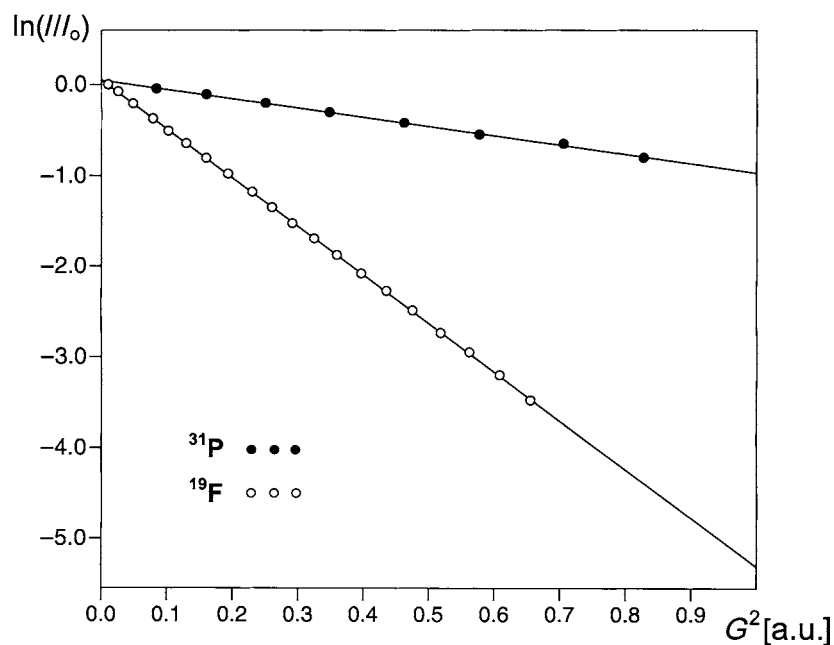


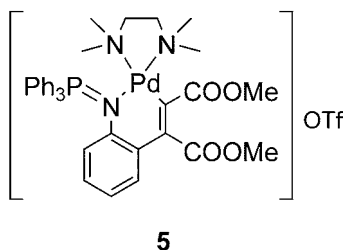
Fig. 7. Plots of $\ln(I/I_0)$ vs. arbitrary units proportional to the square of the gradient amplitude for ^{31}P - (black circles) and ^{19}F - (white circles) PGSE diffusion measurements on a 20 mM CD_3OD solution of Pd hydride **2** at 240 K

Table 6. ^1H -, ^{19}F - and ^{31}P -PGSE Diffusion Results for **2** and **5** in MeOH at 240 K^{a)}

Nucleus	2		5			
	MeOH ^{c)}		MeOH ^{c)}		CD ₃ OD	
	D [$10^{-10} \text{ m}^2 \text{ s}^{-1}$]	r_{H} [Å]	D [$10^{-10} \text{ m}^2 \text{ s}^{-1}$]	r_{H} [Å]	D [$10^{-10} \text{ m}^2 \text{ s}^{-1}$]	r_{H} [Å]
^1H					1.79(6)	6.4(1)
$^1\text{H}^{\text{d)}$					1.78(6)	6.4(1)
$^{31}\text{P}^{\text{d)}$	2.19(6)	5.2(1)	2.10(6)	5.5(1)	1.84(6)	6.2(1)
^{19}F	3.97(6)	2.9(1)	3.86(6) ^{e)}	3.0(1)	3.41(6)	3.4(1)
$^{19}\text{F}^{\text{d)}$	3.97(6)	2.9(1)				

^{a)} 20 mM. ^{b)} η (MeOH) = $1.53 \text{ kg s}^{-1} \text{ m}^{-1}$. ^{c)} Plus three drops of CD_3OD for the lock. ^{d)} Measured with the *Stejskal–Tanner* sequence (Fig. 1,a). As expected, the *Stejskal–Tanner* and the stimulated echo pulse sequences afford identical D values. ^{e)} Average of two measurements that yield $D = 3.83$ and 3.86 .

To have a reference for comparison, and to check the accuracy of the low-temperature ^{31}P -PGSE diffusion experiments, we have carried out some test measurements on the model Pd salt **5** [18][34]. The results are also shown in *Table 6*, from which it can be seen that the ^1H - and ^{31}P -experiments in CD_3OD afford similar D values. To facilitate a comparison with **2**, **5** was also studied in MeOH. Interestingly, we observe larger D values (13–14% bigger) than in CD_3OD .



From our previous work [18] with **5** in CD_3OD at ambient temperature (see *Table 7*), it is clear that the CF_3SO_3^- anion in this compound moves independently of the cation. The ratio $D(\text{anion})/D(\text{cation})$ for **5** at 299 K (1.8–1.9) is identical to that observed for the same compound at 240 K (*Table 6*), so that it can be concluded that, within this temperature range, there is no change in interionic interactions in **5**.

Table 7. D Values and Calculated r_H for **2** and **5** [18] at 299 K^a)

2		5						
MeOH ^{b)} c)		MeOH ^{b)} c)		CD ₃ OD ^{b)}		CD ₂ Cl ₂ ^{d)}		
D [10 ⁻¹⁰ m ² s ⁻¹]	r_H [Å]	D [10 ⁻¹⁰ m ² s ⁻¹]	r_H [Å]	D [10 ⁻¹⁰ m ² s ⁻¹]	r_H [Å]	D [10 ⁻¹⁰ m ² s ⁻¹]	r_H [Å]	
^1H				6.64(6)	6.2(1)	8.42(6)	6.3(1)	
^{19}F	14.22(6)	2.9(1)	13.76(6)	3.0(1)	12.35(6)	3.4(1)	10.81(6)	4.9(1)

^a) 9–10 mm. ^b) η (MeOH) = 0.533 kg s⁻¹m⁻¹. ^c) With a capillary of D₂O for the lock. ^d) η (CH₂Cl₂) = 0.414 kg s⁻¹m⁻¹.

The *ca.* 2.9–3.0-Å r_H value for the CF_3SO_3^- anion in MeOH is similar for both **2** and **5**, as expected for a free-movement situation. However, these calculated r_H values are too large for solvent-free CF_3SO_3^- , pointing to strongly solvated anions.

In retrospect, ^{19}F -PGSE data for **2** and **5** at ambient temperature in MeOH ($D = 14.22$ and 13.76×10^{-10} m² s⁻¹ respectively, *Table 7*) suggested independent motion of the anions. However, these data were clouded by the slow decomposition of **2**, and by the difficulty (for **2**) of comparing them with diffusion data from the cation.

Low-Temperature Diffusion Measurements on 3. The complex $[\text{W}(\text{Cp})(1\text{-adaman- to- tol})(\text{CO})_3](\text{CF}_3\text{SO}_3)$ **3** forms through ionic hydrogenation of the corresponding adamantone by reaction with $[\text{WH}(\text{Cp})(\text{CO})_3]$ and $\text{CF}_3\text{SO}_3\text{H}$ [35]. The crystal structure of the related $[\text{W}(\text{Cp})(\text{CO})_3(\text{HO}^i\text{Pr})](\text{CF}_3\text{SO}_3)$ shows H-bonding between the alcohol OH proton and an O-atom of the CF_3SO_3^- [35]. ^1H -NMR Data for **3**

suggest that this bond is also present in solution [35], and it should be possible to confirm this by ^1H - and ^{19}F -PGSE diffusion measurements on **3**⁶⁾.

However, **3** is not stable at ambient temperature and decomposes within hours to yield free adamantol and $[\text{W}(\text{Cp})(\text{CF}_3\text{SO}_3)(\text{CO})_3]$, **6** [35]. To avoid the ambiguity associated with complexed CF_3SO_3^- in **6**, diffusion data for **3** were obtained at 231 K (in CD_2Cl_2), where no decomposition was observed.

^1H and ^{19}F Diffusion data for two different samples of **3** are given in Table 8. To confirm that convection is minimal, measurements with three different Δ values were made. In contrast to the observations for **2** (in MeOH), the CF_3SO_3^- anion in **3** (in CD_2Cl_2) moves at the same rate as the W-cation. Moreover, the calculated r_{H} value for the anion in **3** (4.6–4.7 Å) is much larger than in **2** (2.9 Å), clearly indicating association to the cation in **3**. We assign the observed equivalence of D values for cation and anion in **3** to the presence of H-bonding between them.

Table 8. ^1H - and ^{19}F -PGSE Diffusion Results for **3** and **5** in CD_2Cl_2 at 231 K^{a,b)}

Nucleus	Δ (ms)	3 ^{c)}		5	
		D [$10^{-10} \text{ m}^2 \text{ s}^{-1}$]	r_{H} [Å]	D [$10^{-10} \text{ m}^2 \text{ s}^{-1}$]	r_{H} [Å]
^1H	118	3.88(6), 3.87(6)	4.7(1)	2.83(6)	6.4(1)
	168	3.91(6), 3.90(6)	4.6(1)		
	268	3.93(6), 3.95(6)	4.6(1)	2.77(6)	6.5(1)
^{19}F	118	3.87(6), 3.84(6)	4.7(1)	3.72(6)	4.9(1)
	168	3.84(6), 3.89(6)	4.7(1)		
	268	3.95(6), 3.94(6)	4.6(1)	3.79(6)	4.8(1)

^{a)} 10 mm. ^{b)} η (CH_2Cl_2) = 0.933 $\text{kg s}^{-1} \text{ m}^{-1}$. ^{c)} The results from two different samples (left and right columns) prepared under similar conditions are shown.

Again, to have a reference for comparison, we carried out some additional low-temperature measurements on the Pd salt **5** in CD_2Cl_2 , and these results are also shown in Table 8. From our previous studies with **5** [18] (see Table 7), we have established that, in CD_2Cl_2 and at 299 K, there is partial ion-pairing between the cation and anion in this compound. This results in a calculated r_{H} for the CF_3SO_3^- anion (at 299 K) of 4.9 Å in CD_2Cl_2 is considerably larger than the 3.4 Å value obtained in CD_3OD at the same temperature. The ratio $D(\text{anion})/D(\text{cation})$ for **5** in CD_2Cl_2 at 299 K (1.3, from Table 7) is very close to that observed from the low-temperature (231 K) D values in Table 8, so that it can be concluded that at 231 K the degree of ion-pairing in **5** has not changed with respect to ambient temperature.

The D values for both **3** and **5** at 231 K (Table 8) reflect negligible influence of convection and excellent reproducibility.

Conclusions. – We have found a convenient experimental set-up to eliminate convection from low-temperature PGSE diffusion measurements. We suggest that correct D values and temperature-independent r_{H} can be obtained with an appropriate insert. Low-temperature ^1H -, ^{19}F -, and ^{31}P -PGSE diffusion measurements on the

⁶⁾ The presence of a H-bond interaction between cation and anion would be reflected in similar D values for both in CD_2Cl_2 , where, otherwise, they would be only partially ion-paired (see, for instance, [16,b]).

relatively unstable Pd catalyst **2** in MeOH, reveal no cation-anion interaction, while for the sensitive W adamantol complex **3**, in CH₂Cl₂, we have confirmed the presence of a strong H-bond from the CF₃SO₃⁻ to the alcohol H-atom of 1-adamantol.

Experimental Part

Complexes **3** [35], **5** [34], and **6** [33] have been kindly provided by other groups. Complex **4** was available in our laboratory.

All measurements were performed on a Bruker AVANCE spectrometer (300, 400 MHz) equipped with a microprocessor-controlled gradient unit and a multinuclear probe (normal or inverse) with an actively shielded Z-gradient coil. The shape of the gradient pulse was rectangular, and its strength varied automatically in the course of the experiments.

The calibration of the gradients on each spectrometer was carried out *via* a diffusion measurement of HDO in D₂O at ambient temp. The *D* value of each sample can then be calculated according to Eqn. 3, where $D_{\text{HDO}} = 1.9 \times 10^{-9} \text{ m}^2 \text{ s}^{-1}$ [35].

$$D = \frac{m_i \times D_{\text{HDO}}}{m_{\text{HDO}}} \quad (3)$$

In Eqn. 3, m_i is calculated for each measurement from the observed slope, m_{obs} , with the help of Eqn. 4, which takes into account the settings for the diffusion delay Δ , the gradient length δ , as well as the nature of the observed nucleus X, with respect to the calibration with HDO (where $\Delta = 167.75 \text{ ms}$ and $\delta = 1.75 \text{ ms}$).

$$\frac{m_{\text{obs}}}{m_i} = \left(\frac{\gamma_x}{\gamma_{\text{H}}}\right)^2 \left(\frac{\delta_x}{\delta_{\text{HDO}}}\right)^2 \frac{\left(\Delta - \frac{\delta}{3}\right)_x}{\left(\Delta - \frac{\delta}{3}\right)_{\text{HDO}}} \quad (4)$$

Unless otherwise stated, for all the ¹H and ¹⁹F experiments, $\delta = 1.75 \text{ ms}$. The Δ values given in the Tables as 68, 118, 218, 318... ms are really 67.75, 117.75, 217.75, 317.75... ms. The gradient strength was usually incremented in 3- or 4 % steps, so that 15–25 points could be used for regression analysis. The number of scans per increment varied between 4 and 16 from one sample to another, according to the concentration and the volume in the NMR tube. Typical exper. times were around 0.5–1 h. Sample concentrations are noted in the Tables.

For the low-temperature ³¹P-PGSE measurements, $\delta = 5–7 \text{ ms}$ and $\Delta = 43–48 \text{ ms}$. The evolution time before and after the 180° pulse was set to 29 ms in all experiments (although this was necessary only for **2**); 8–9 points were acquired, with 250–520 scans for **5** and 1200 scans for **2**. The exper. time per increment was 1–2 h. *T*₁ values for ³¹P were close to 1s, so that a relaxation delay of 5–7 s was used.

All data leading to the reported *D* values afforded lines with correlation coefficients > 0.999.

Jerschow *et al.* [24] have suggested the use of a double stimulated echo (DSTE) pulse sequence to eliminate convection artifacts, and successfully applied this method at high temp. (although they state that its utility is limited to convection currents with a constant laminar-flow profile during the diffusion interval, and that it does not compensate turbulent convection). Our efforts to implement this sequence on our low-temp. measurements afforded nonlinear plots as in Fig. 2. Consequently, all measurements have been carried out with the stimulated echo pulse sequence (Fig. 1, b), with the exception of those marked with an asterisk in Table 6, which employ the Stejskal–Tanner sequence (Fig. 1, a).

To eliminate convection in the low-temp. NMR measurements we have used two commercially available coaxial NMR tubes, as shown in Fig. 3. The inner and outer tubes are separated by a pyrex spacer suitable for variable-temp. experiments. A space of ca. 5 mm is left between both tubes at the bottom. The experiments on **2** (at low temperature) were carried out with the *M* insert, and the measurements on **3** with the *S* insert. No decomposition was observed during the experiments, not even during the long ³¹P measurements on **2**. The precise temps. were measured with a thermocouple introduced inside the bore of the magnet.

With the (*L*) insert, convection was not completely eliminated and Δ -dependent *D* values were obtained. However, we have not observed a variation of *D* with δ (the gradient pulse length). Four measurements on **4** in CD₂Cl₂ with $\Delta = 68$ ms and $\delta = 1.75, 2.5, 3.5$ and 4.0 ms afforded similar *D* values of 4.77, 4.70, 4.73, and $4.78 \times 10^{-10} \text{ m}^2 \text{ s}^{-1}$, respectively (measured with (*L*) and air in the intermediate space between the tubes).

We have also tested the use of a smaller capillary (stem coaxial insert), with a sample capacity of 530 μl , but we finally discarded it, as difficulties in shimming resulted in broad signals that sometimes even could not be measured. The low signal-to-noise ratio was an additional problem of this configuration. Moreover, in measurements with **4** in CD₂Cl₂, we could not detect a significant improvement with respect to (*S*), even for long diffusion delays ($\Delta = 418$ ms).

P. S. P. thanks the *Swiss National Science Foundation*, and the *ETH Zürich* for financial support. *E. M.-V.* thanks the *Seneca Foundation (Comunidad Autónoma de la Región de Murcia, Spain)* for a grant. Special thanks are due to Prof. *B. T. Heaton* for the gift of **6**, Prof. *R. M. Bullock* for the gift of **3**, and Prof. *J. Vicente*, Dr. *J. A. Abad* and *J. López-Serrano* for the gift of **5**. We would also like to thank Dr. *Heinz Rüegger* and *Felix Bangerter* (ETH, Zürich) for very helpful discussions and advice.

REFERENCES

- [1] W. S. Price, *Ann. Rep. NMR Spectrosc.* **1996**, 32, 51.
- [2] P. Stilbs, *Prog. NMR Spectrosc.* **1987**, 19, 1.
- [3] A. Pichota, P. S. Pregosin, M. Valentini, M. Wörle, D. Seebach, *Angew. Chem.* **2000**, 112, 157.
- [4] C. B. Gorman, J. C. Smith, M. W. Hager, B. L. Parkhurst, H. Sierzputowska-Gracz, C. A. Haney, *J. Am. Chem. Soc.* **1999**, 121, 9958.
- [5] T. Geldbach, P. S. Pregosin, A. Albinati, F. Rominger, *Organometallics* **2001**, 20, 1932.
- [6] D. Drago, P. S. Pregosin, A. Pfaltz, *Chem. Commun.* **2002**, 286.
- [7] A. Burini, J. P. Fackler, R. Galassi, A. Macchioni, M. A. Omary, M. A. Rawashdeh-Omary, B. R. Pietroni, S. Sabatini, C. Zuccaccia, *J. Am. Chem. Soc.* **2002**, 124, 4570.
- [8] A. Macchioni, C. Zuccaccia, E. Clot, K. Gruet, R. H. Crabtree, *Organometallics* **2001**, 20, 2367.
- [9] S. Beck, A. Geyer, H. H. Brintzinger, *Chem. Commun.* **1999**, 2477.
- [10] B. Olenyuk, M. D. Lovin, J. A. Whiteford, P. J. J. Stang, *J. Am. Chem. Soc.* **1999**, 121, 10434.
- [11] R. M. Stoop, S. Bachmann, M. Valentini, A. Mezzetti, *Organometallics* **2000**, 19, 4117.
- [12] E. J. Cabrita, S. Berger, *Magn. Reson. Chem.* **2001**, 39, S142.
- [13] R. K. Harris, K. A. Kinnear, G. A. Morris, M. J. Stchedroff, A. Samadi-Maybadi, *Chem. Commun.* **2001**, 2422.
- [14] K. R. Deaton, E. A. Feyen, H. J. Nkulabi, K. F. Morris, *Magn. Reson. Chem.* **2001**, 39, 276.
- [15] N. E. Schlörer, E. J. Cabrita, S. Berger, *Angew. Chem., Int. Ed.* **2002**, 41, 107.
- [16] a) M. Valentini, P. S. Pregosin, H. Rüegger, *Organometallics* **2000**, 19, 2551; b) M. Valentini, P. S. Pregosin, H. Rüegger, *J. Chem. Soc., Dalton Trans.* **2000**, 4507; c) M. Valentini, H. Rüegger, P. S. Pregosin, *Helv. Chim. Acta* **2001**, 84, 2833; d) Y. Chen, M. Valentini, P. S. Pregosin, A. Albinati, *Inorg. Chim. Acta* **2002**, 327, 4.
- [17] a) C. Zuccaccia, G. Bellachioma, G. Cardaci, A. Macchioni, *Organometallics* **2000**, 19, 4663; b) G. Bellachioma, G. Cardaci, F. D'Onofrio, A. Macchioni, S. Sabatini, C. Zuccaccia, *Eur. J. Inorg. Chem.* **2001**, 1605; c) B. Binotti, G. Bellachioma, G. Cardaci, A. Macchioni, C. Zuccaccia, E. Foresti, P. Sabatino, *Organometallics* **2002**, 21, 346; d) G. Bellachioma, B. Binotti, G. Cardaci, C. Carfagna, A. Macchioni, S. Sabatini, C. Zuccaccia, *Inorg. Chim. Acta* **2002**, 330, 44.
- [18] E. Martínez-Viviente, H. Rüegger, P. S. Pregosin, J. López-Serrano, *Organometallics* **2002**, 21, 5841.
- [19] E. Martínez-Viviente, P. S. Pregosin, *Inorg. Chem.* **2003**, 42, 2209.
- [20] D. G. Blackmond, A. Lightfoot, A. Pfaltz, T. Rosner, P. Schnider, N. Zimmermann, *Chirality* **2000**, 12, 442.
- [21] R. Kato, T. Terao, T. Seimiya, *Langmuir* **1994**, 10, 4468.
- [22] A. Jerschow, N. Müller, *J. Magn. Reson.* **1997**, 125, 372.
- [23] N. Hedin, I. Furó, *J. Magn. Reson.* **1998**, 131, 126.
- [24] N. Hedin, T. Y. Yu, I. Furó, *Langmuir* **2000**, 16, 7548.
- [25] O. Mayzel, Y. Cohen, *J. Chem. Soc., Chem. Commun.* **1994**, 1901.
- [26] O. Mayzel, O. Aleksyuk, F. Grynszpan, S. E. Biali, Y. Cohen, *J. Chem. Soc., Chem. Commun.* **1995**, 1183.
- [27] L. Frish, M. O. Vysotsky, S. E. Matthews, V. Böhmer, Y. Cohen, *J. Chem. Soc., Perkin Trans. 2* **2002**, 8.
- [28] L. D. Landau, E. M. Lifshitz, 'Fluid Mechanics', Pergamon, Oxford, 1987.

- [29] A. Bejan, 'Convection Heat Transfer', Wiley, New York, 1995.
- [30] P. T. Callaghan, 'Principles of Nuclear Magnetic Resonance Microscopy', Clarendon, Oxford, 1991.
- [31] J. T. Edward, *J. Chem. Educ.* **1970**, *47*, 261.
- [32] C. L. Yaws, 'Chemical Properties Handbook', McGraw-Hill, 1999 (online: <http://www.knovel.com>).
- [33] a) W. Clegg, G. R. Eastham, M. R. J. Elsegood, R. P. Tooze, X. L. Wang, K. W. Whiston, *Chem. Commun.* **1999**, 1877; b) G. R. Eastham, B. T. Heaton, J. A. Iggo, R. P. Tooze, R. Whymann, S. Zacchini, *Chem. Commun.* **2000**, 609; c) W. Clegg, G. R. Eastham, M. R. J. Elsegood, B. T. Heaton, J. A. Iggo, R. P. Tooze, R. Whymann, S. Zacchini, *J. Chem. Soc., Dalton Trans.* **2002**, *17*, 3300.
- [34] J. Vicente, J. A. Abad and J. López-Serrano, Grupo de Química Organometálica, Departamento de Química Inorgánica, Universidad de Murcia, Murcia, Spain. Unpublished results.
- [35] J.-S. Song, D. J. Szalda, R. M. Bullock, *Organometallics* **2001**, *20*, 3337.
- [36] H. J. W. Tyrrell, K. R. Harris, 'Diffusion in Liquids', Butterworths. London 1984.

Received March 12, 2003